Global Ecology and Conservation 19 (2019) e00687

Contents lists available at ScienceDirect

Global Ecology and Conservation

journal homepage: http://www.elsevier.com/locate/gecco

Original Research Article

Using N-mixture models to estimate abundance and temporal trends of black rhinoceros (*Diceros bicornis* L.) populations from aerial counts

Zaara Kidwai [a, d], Jose Jimenez [b, *], Cornelius J. Louw [a], H.P. Nel [c], Jason P. Marshal [d]

[a] School of Environmental Sciences at the University of South Africa (UNISA), PO Box 392, South Africa
[b] Instituto de Investigación en Recursos Cinegéticos (IREC, CSIC-UCLM-JCCM), Ronda de Toledo s/n, Ciudad Real, Spain
[c] North West Parks and Tourism Board, PO Box 4488, Mmabatho, 2735, South Africa, HPN
[d] Centre for African Ecology, School of Animal, Plant and Environmental Sciences, University of the Witwatersrand, Private Bag 3 Wits, Johannesburg, 2050, South Africa

ARTICLE INFO

Article history:
Received 28 January 2019
Received in revised form 23 April 2019
Accepted 9 June 2019

Keywords:
Aerial survey
Black rhinoceros
Dynamic N-Mixture models
South Africa

ABSTRACT

Inaccurate estimates of animal populations may lead to flawed management interventions, therefore, it is essential to understand the status and population trend of a species in order to plan its management efficiently. Aerial surveys are considered a useful method for estimating the population size of large conspicuous animals inhabiting large areas, but raw count data from aerial surveys usually underestimate population sizes due to imperfect detection. The use of N-mixture models with aerial count data provides a useful tool to estimate the population sizes while taking detection probability into account. As a study case we used aerial surveys conducted for monitoring black rhinoceros (*Diceros bicornis*) in Madikwe Game Reserve and Pilanesberg Nature Reserve (South Africa) during 1999–2015, and we analysed data with a dynamic extension of the N-mixture model. We estimated 0.078–0.098 and 0.139–0.142 individuals/km^2, respectively, and we found evidence for density dependence in both reserves with a carrying capacity of 0.122 (0.102–0.142) individuals/100 km^2. Based on simulations used to assess precision of the estimates, root-mean-square error model (RMSE) estimates was significantly smaller than those for the raw maximum counts.
The N-mixture models provide a promising approach to estimate population size, trends and demographic characteristics of large conspicuous mammals such as black rhinoceroses. Such analysis can provide estimates that are more accurate than raw counts. In addition, use of model covariates that affect a species' population parameters can provide useful information for their conservation and management.

1. Introduction

Reliable information on the status of animal populations is essential to inform decision-making processes, assess the degree of compliance with planned conservation and management goals, or avoid undesirable outcomes from interventions

* Corresponding author.
E-mail addresses: zaarakidwai@gmail.com (Z. Kidwai), Jose.Jimenez@uclm.es (J. Jimenez), louwcj@unisa.ac.za (C.J. Louw), hpnel@mweb.co.za (H.P. Nel), Jason.Marshal@wits.ac.za (J.P. Marshal).

https://doi.org/10.1016/j.gecco.2019.e00687

(McCarthy and Possingham, 2007; Nichols and Williams, 2006). Inaccurate population estimates can lead to errors in establishing population status and setting conservation goals that limit the ability to determine the effects of management actions (Wiest et al., 2018). However, knowledge of population sizes, especially for those animals that are elusive or distributed over large areas at low density, can be technically difficult or costly to obtain (Skalski, 1994). In such cases, given that there are limited resources for monitoring wildlife populations, there is a need for effective and cost-efficient survey methods (Parker et al., 2011).

Species of African rhinoceroses, the white rhino (*Ceratotherium simum*) and the black rhino (*Diceros bicornis*), are prime examples of this challenge. They typically occur at low density in protected areas administered by government and private owners (Walpole et al., 2001). The black rhino, in particular, is among the ungulates that are threatened globally (Ferreira et al., 2017). The species is classified as "critically endangered" (Emslie, 2012) because of the demand for rhino horn, mainly from Far Eastern markets (Martin, 1991). Although intraspecific variation among black rhinos is still on debate (Moodley et al., 2017), of the 7-8 originally described subspecies, three have been declared "extinct" by the International Union for Conservation of Nature (IUCN) (Amin et al., 2006; Emslie, 2012). Over the last two decades, the remaining subspecies have been declining throughout the continent (Amin et al., 2006) despite anti-poaching efforts (Cromsigt et al., 2002; Gakahu, 1993; Hrabar and du Toit, 2005).

The conservation status of the South African subspecies is still a key concern (Cromsigt et al., 2002; Ferreira et al., 2017). In 1930, there were an estimated 110 individuals of *D. b. minor* in South Africa in two populations: Hluhluwe-iMfolozi Park and Mkhuze Game Reserve, KwaZulu-Natal province. With protection, active management and translocations to expand range and numbers, by the end of 2015 there were 54 breeding populations conserving an estimated 1580 animals (Emslie and Adcock, 2016). However, a subsequent upsurge of poaching began in 2008, and *D.b.minor* has suffered the highest poaching (551 reported) for the period 2010-2017, compared to 260 for the equally abundant *D.b.bicornis* and 134 for the rarer *D.b.michaeli* (Southern African Development Community Rhino Management Group (SADC RMG), personal communication, April 4, 2019).

Continued monitoring of black rhino populations is needed not only to evaluate the efficiency of anti-poaching efforts, but also to provide information on population dynamics. In black rhinos, density-dependent social constraints such as territorial and antagonistic behaviours (Adcock, 1994) contribute to population regulation (Hanski, 2006; Lundberg et al., 2000; Sæther, 1997). Resource availability per individual is reduced at high population densities, which affects survival, natality and age at maturity (Hrabar and du Toit, 2005; Sæther, 1997). In addition, many rhino populations are small and fragmented: ca. 75% of the reserves in Kenya, Namibia, and South Africa have <50 animals (Berger, 1994) such that genetic diversity loss and environmental stochasticity are serious threats (Hrabar and du Toit, 2005; Mduma et al., 1999; Owen-Smith, 1990; Sinclair et al., 1985). Black rhino conservation practices typically seek to maximise the population growth by relying on a metapopulation structure (Ferreira et al., 2017; Foose et al., 1993; Hrabar and du Toit, 2005). This requires detailed knowledge of population size, trend and demographic rates.

The status of rhinoceros populations is commonly monitored by individual identification (ID) based methods developed by SADC RMG (e.g. to provide information on mortalities, calving, removals, poaching, individuals missing and presumed dead). ID-based monitoring is recommended for black rhinos given the additional value of demographic data that can be obtained. However, intensive helicopter block counts are more common for population estimation of large mammals in areas where ID-based monitoring is not logistically feasible. (Caughley, 1977; Brockett, 2002; Ferreira et al., 2017, 2011; Williams et al., 2017). Detection probability of animals, however, can be highly variable and is always lower than one. Use of raw count data from aerial surveys, therefore, usually underestimates population size (Caughley, 1977; Steinhorst and Samuel, 1989). Many authors have developed procedures for estimating visibility bias and corrections to population estimators (Hone, 2008; Jachmann, 2002; King et al., 1985; Ottichilo, 1999), and these are also used in aerial surveys of black rhinos (Ferreira et al., 2011; Mackie et al., 2013). Moreover, overestimation of abundance can occur from double-counting or false positives (Schmidt, 2005) which can also underestimate survival probabilities in relation to environmental covariates (Gimenez et al., 2008; MacKenzie et al., 2006; Martin et al., 1995; Nichols and Williams, 2006; Tyre et al., 2003) while overestimating the extinction and turnover rates (Moilanen, 2002; Nichols et al., 1998).

In this study, we used data from aerial surveys of black rhinos, conducted in two reserves, Pilanesberg and Madikwe, South Africa, to estimate the population sizes and temporal trends between 1999 and 2015. To accommodate imperfect detection, we used N-mixture models that estimate abundance and detection probability simultaneously without identification of individuals in the populations (Royle, 2004). N-mixture models are rarely used with aerial count data in South Africa to estimate wildlife abundance (but see Lyet et al., 2016). The objective of this study was to demonstrate the use of N-mixture models to improve precision of abundance estimates, and comparing those results with established estimates from RMG ID-based monitoring methods.

2. Material and methods

2.1. Study sites

Madikwe Game Reserve (henceforth Madikwe) is approximately 60 000 ha in extent and is one of the largest game reserves in South Africa. It is situated close to the Botswana border in the far north of North West Province (24° 45′S 26° 16′E). The vegetation of the reserve is composed of large open woodlands and grasslands, divided by the "Rant van Tweedepoort"

Hills in the middle of the reserve, and bordered by the Dwarsberg Mountains in the south (NWPTB, 2018). The majority of the reserve is "Sourish Mixed Bushveld" (Acocks, 1975), with a tree-shrub layer of medium-low to medium-high growth and tall-growing *Vachellia* (previously *Acacia*) species being the most dominant (Fig. 1). The main features of this area are the scattered inselbergs or isolated hills abruptly rising from otherwise flat plains (NWPTB, 2018). The climate in this region can be divided into a rainy season (October–April) and a dry season (May–September). The area receives rainfall of <500 mm per annum and range in temperatures in the reserve is 3 °C–32 °C (NWPTB, 2018). The reserve is a home to around 66 large mammalian species including lion (*Panthera leo*), leopard (*Panthera pardus*), rhinoceros (both black and white), elephant (*Loxodonta africana*) and African buffalo (*Syncerus caffer*); along with more than 300 species of resident and migrant birds. Black rhinos were reintroduced in the area in 1992.

Pilanesberg Nature Reserve (henceforth Pilanesberg; 25° 15′ 42.12"S, 27° 6′ 2.88"E) covers an area of 55 000 ha and is situated in the Bojanala Region of the North West Province. Geologically, the area is formed by a crater of a long-extinct volcano that was produced by volcanic eruptions *ca.* 1300 million years ago and fringed by a few concentric ridges or rings of hills (Carruthers, 2011). The park is in the transition zone between the dry Kalahari and wetter low-veld vegetation, commonly referred to as "Sour Bushveld" (Acocks, 1975). The habitat comprises *Vachellia* and broad-leaf bushveld species, varying from open grassland to thickets (Hrabar and du Toit, 2005) (Fig. 1). The reserve receives annual rainfall in the range of 600–700 mm, with most of that falling during a dominant rainy season (October–April) followed by dry season from May to September. Highly variable annual rainfall can produce frequent droughts in some years (Farrell et al., 1978; McCarthy and Rubidge, 2006; Mucina and Rutherford, 2006; Carruthers, 2011). The average annual temperature in the area ranges from 15 °C to 30 °C (NWPTB, 2018). About twenty four species of the large mammals occur in Pilanesberg including lion, leopard, elephant, black and white rhino, buffalo, springbok (*Antidorcas marsupialis*), brown hyena (*Hyaena brunnea*), impala (*Aepyceros melampus*), cheetah (*Acinonyx jubatus*), sable antelope (*Hippotragus niger*), giraffe (*Giraffa camelopardalis*), plains zebra (*Equus quagga*), hippopotamus (*Hippopotamus amphibious*) and crocodile (*Crocodylus niloticus*). Nineteen black rhinos were reintroduced to Pilanesberg 1981-1983 and a further five animals were added in 1989 (Adcock et al., 1998). A recent increase in rhino poaching has been described in this area (NWPTB, 2015).

The black rhino populations in Madikwe and Pilanesberg both are considered by the IUCN "Key": critical for the survival of the species, in the type "Key 2": population increasing or stable and N = 51-100 (Brooks and Emslie, 1999).

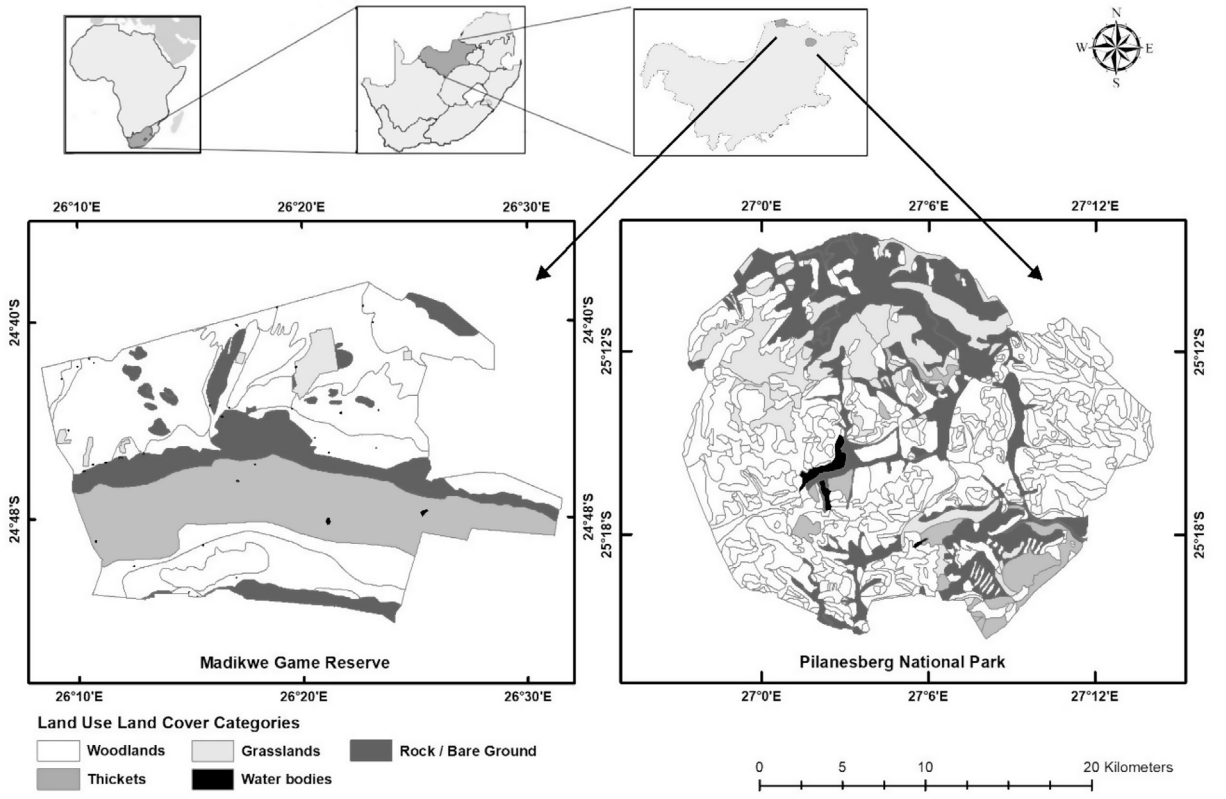

Fig. 1. Details of geographic locations and land use land cover (LULC) categories in the study sites (NWPTB, 2018).

2.2. Data collection

Three annual replicate aerial surveys were conducted 1999-2015 during the late dry period (July–October) by using a four-seat Bell Jet Ranger II helicopter with all doors removed. The time between two consecutive replicate surveys varied between 1 and 7 days. The survey team consisted of a pilot, a data recorder and one observer on each side. The survey covered the entire area of both the reserves by flying 500 m wide transects, at 90 km/h and 60–100 m above ground (Nel, 2015). Data recorded included locations of all observed individuals, date and time of each observation, and flight time of the survey summed over by year.

2.3. Data analysis

We used an N-mixture model to estimate species abundance from count data while accounting for imperfect detection (Royle, 2004). This model depends on data from survey counts that are replicated both in space and over time (Kéry et al., 2009) which are necessary to enabled estimation of detection probability. This information is used to get the real abundance (λ) from a local variation in the abundance (Ni) at i sites using j temporal counts. There are two linked processes:

1. Ecological. The species has a local abundance in i sites (N_i) with latent abundance λ that is described by a Poisson distribution

$$Ni \sim Poisson(\lambda)$$

2. Observation. We observed y_{ij} (counts) from the N_i (individuals in each i sites) in each j temporal replicates with a detection probability p, which is described by a binomial distribution:

$$y_{i,j} \mid N_i \sim \text{Binomial}(N_i, p)$$

Thus, the N-mixture model simply consist of two linked generalized linear models. Inputs to the model are the replicate counts, which then yields estimates of the parameters of the ecological (abundance) and the observation processes (detection probability) (Kéry and Schaub, 2012). In this study we used a dynamic N-mixture or multi-season model that is a robust robust-design generalized form of N-mixture model (Royle, 2004) for open populations (Dail and Madsen, 2011). The covariates we used in the model are those that could influence the detection process: survey effort (total flight duration per year), Julian date (with a quadratic term), site (as a factor, characterizing different reserves) and the interaction terms. For population growth rate, we used climate covariates: annual rainfall and temperature (NASA, 2018) (Table 1).

We began by assessing the assumptions of the N-mixture model. The first is that the population is geographically and demographically closed within the replicates in a year and a given site (in this case, a reserve). In our study, primary periods were years, over which the population was assumed to be open to gains and losses, while the three annual replicate surveys (secondary periods) were obtained within a sufficiently short time that the local population was assumed to be closed to births, deaths and movement. The second assumption is that individuals are counted only once per survey. Third, animal detections are independent of each other; otherwise, this issue must be addressed using a beta-binomial rather than a binomial observation model (Martin et al., 2011) that account for correlated detections of individuals. Finally, density dependence in vital rates, if present, must be explicitly modelled (Bellier et al., 2016) to consider this specific dynamic. Based on the biology of black rhinos, the fenced nature of the reserves, and methods of data capture, the first three assumptions are likely reasonable, although limited double-counting could lead to the estimation (Link et al., 2018). Moreover, we considered density dependence that could potentially exist (Hanski, 2006; Hrabar and du Toit, 2005; Lundberg et al., 2000; Sæther, 1997). Bellier et al. (2016) described the bias that may occur with density dependence and environmental stochasticity when estimating survival and recruitment, and they compared the use of four Dail-Madsen models in a Bayesian approach: 1) no density dependence (DM), 2) density dependence on survival (DDS), 3) density dependence on recruitment (DDR) and 4)

Table 1
Covariates used to model abundance, recruitment, survival (or growth rate) and probability of detection using a binomial mixture model in Pilanesberg and Madikwe (South Africa), 1999–2015.

Covariate	Sample-unit specific measurement	Mean	Range	Rationale
Site	Factor	–	–	We can expect different detection probability between sites, due to vegetation cover and geomorphological attributes
Climate	Average annual rainfall (mm)	547.8	268.5–835.8	Inter-calving intervals decreased with an increase in rainfall (Berkeley and Linklater, 2010; Hrabar and du Toit, 2005). We can expect changes in recruitment
	Average annual temperature (°C)	20.8	19.0–22.6	A positive relationship was observed between the percentage of calves born each month and mean monthly temperature (Freeman et al., 2014)
Fly time	Hours of flight (site by year)	19.6	14.1–24.0	As time of flight increase, we can expect the detection of black rhino also increase
Julian date	Ordinal day of the year	235	205–287	We can expect a variation in detection in the time of year counts were conducted (Brockett, 2002)

density dependence on both survival and recruitment (DDSR). To assess these models, they performed simulations, and adjusted the four models using cross-simulations. Bellier et al. (2016) concluded that accurate estimates of abundance and detection probability were possible without accounting for density dependence, but that recruitment, growth rate, or survival would be biased without explicitly modelling the density-dependent process.

To fit the N-mixture model, we used the unmarked package (Fiske and Chandler, 2011) in R (R Core Team, 2018), which provides a unified modelling framework for hierarchical models. It has been developed to separately model an effect of explanatory variables on both latent abundance and occurrence, as well as on a conditional detection process. Unmarked also includes tools for data exploration, model fitting, model criticism, post-hoc analysis, and model comparison (Fiske and Chandler, 2011). The computational cost of analysing models using unmarked is significantly lower than using the Bayesian approach.

Data were modelled using maximum likelihood methods with the function pcountOpen, specifically written to handle the Dail and Madsen model in unmarked (Chandler and King, 2011). For model selection, we followed a three-step process (Hostetler and Chandler, 2015) using the Akaike Information Criteria (AIC) (Akaike, 1974) corrected for small sample sizes (AICc) (Burnham and Anderson, 2002). First, we selected three models of initial abundance for the response variable (count data) by comparing the performance of Poisson, zero-inflated Poisson and Negative Binomial models. Second, we compared a set of candidate models with covariates that might affect the detection process. Third, we compared between four possible models with different population dynamics from unmarked: constant, trend, auto-regressive and Ricker and Gompertz models. Ricker and Gompertz models allowed us to evaluate density dependence (Hostetler and Chandler, 2015), although the authors warn about the need for additional studies on their validity in certain cases. The Ricker model (Ricker, 1958, 1954) is a discrete population model that gives the expected number (or density) of individuals $N_{t,}$ in year t as a function of the number of individuals in the previous year:

$$N_{[i,t]} = N_{[i,t-1]} \cdot e^{\gamma\left(1-\frac{N_{[i,t-1]}}{\omega}\right)}$$

where gamma (γ) is the maximum instantaneous population growth rate. Omega (ω) is either a parameter that describe the apparent survival rate (deaths and emigrations) in constant, trend and autoregressive models, or the equilibrium abundance (carrying capacity) in density-dependent models. The models require an integer value specifying the upper bound used in the integration (K). In our study, this upper bound was set at $K = 130$, large enough so that it did not affect the model results.

We estimated annual abundance using empirical Bayes methods (ranef) from unmarked and demographic parameters using the best-supported models (based on AIC comparisons) following the rules of $\Delta AIC < 2$ asserted by Burnham and Anderson (2002) to make a multimodel inference on coefficients. We used the predict function from unmarked to produce plots of estimated relationships with the predictors for each covariate. We used the parametric bootstrap approach to obtain p-values from sums of squares (SSE), Chi-square and Freeman-Tukey fit statistics that quantified the fit of a model to a data set, and as a measure of the goodness of fit of the N-mixture selected model. We simulated 1000 bootstrap samples for each fit assessment. A dispersion parameter ($\hat{c}$) was calculated as the ratio of the observed fit statistic to the mean of the simulated distribution. Because the evidence of different density-dependence types, we compared our results in unmarked with the approach from Bellier et al. (2016). Based on the previous knowledge of the black rhino, we can expect density-dependent survival and recruitment (DDSR) (Hanski, 2006; Hrabar and du Toit, 2005; Lundberg et al., 2000; Sæther, 1997). We fitted this specific model using Nimble (De Valpine et al., 2017; NIMBLE Development Team, 2018) to compare results in DDSR model and in unmarked.

We also used N-mixture simulations to test the reliability of our results, show the relationship between the number of spatial replicates (sites) and accuracy of parameters estimates, and to compare the model outputs with the raw data (maximum counts). We employed modified versions of the original scripts from Chandler (2018). To simulate populations we used similar parameters to those obtained from the null models using our data in two different population dynamics scenarios: Ricker ($\lambda = 62$; $\gamma = 0.2$; $\omega = 88$; $p = 0.6$) and constant ($\lambda = 58$; $\gamma = 21$; $\omega = 0.73$; $p = 0.6$) with 2, 5 and 10 spatial replicates (sites). We also compared the population average from 1999 to 2015 in Madikwe and Pilanesberg using the N-mixture approach and ID monitoring from SADC RMG (personal communication, April 4, 2019), assuming those ID estimates were not biased. In the Results we present estimates and 95% confidence intervals (CI), unless otherwise stated.

3. Results

3.1. Model selection

For initial abundance, the negative binomial distribution was more strongly supported than the Poisson and zero-inflated Poisson (Table 2A). The best-supported models for detection included the covariates Site, Julian Date (including the quadratic term) and the interaction term Site x Julian Date (Table 2B). Models with density-dependent dynamics were better supported than constant, trend, or autoregressive models. The best-supported full model was a Ricker model with Rainfall as covariate for growth rate (Table 2C). All models of Table 2C were used for multimodel inference on coefficients (Table 3). Complete R codes and data are in Appendices A and B.

Table 2
Model selection results. A) Initial abundance; B) Detection probability and C) Dynamics selection. Number of sites = 2. Number of years = 17 Covariates considered: Rainfall (R), Temperature (T), Site (Site), Fly time (Ft) and Julian Date (Jd). Model selection based on Akaike's Information Criterion (AIC), number of parameters (nPars), the difference AICc from the best fit models (ΔAICc<2), model weights (AICwt), and cumulative model weights (cltvWt).

	nPars	AIC	ΔAICc	AICwt	cltvWt
A. Initial Abundance					
Negative Binomial $\lambda(.)\gamma(.)\omega(.)$ [Const.]$p(.)$	5	684.37	0	0.95	0.95
Poisson $\lambda(.)\gamma(.)\omega(.)$[Const.]$p(.)$	4	690.74	6.37	0.04	0.99
ZIP $\lambda(.)\gamma(.)\omega(.)$[Const.]$p(.)$	5	692.75	8.38	0.01	1
B. Detection Probability					
$\lambda(.)\gamma(.)\omega(.)$[Const.]$p$(Site + Jd + I(Jd2)+Site*Jd)	9	645.09	0	0.71	0.71
$\lambda(.)\gamma(.)\omega(.)$[Const.]$p$(Site + Jd + I(Jd2)+Site*Jd + Ft)	10	646.90	1.81	0.29	0.99
$\lambda(.)\gamma(.)\omega(.)$[Const.]$p$(Site + Jd + I(Jd2)	8	655.09	10.01	0.01	1
C. Dynamics					
$\lambda(.)\gamma(R)\omega(.)$[Ricker]$p$(Site + Jd + I(Jd2)+Site*Jd)	10	642.70	0.00	0.46	0.46
$\lambda(.)\gamma(R + T)\omega(.)$[Ricker]$p$(Site + Jd + I(Jd2)+Site*Jd)	11	644.47	1.77	0.19	0.65
$\lambda(.)\gamma(.)\omega(.)$[Const]$p$(Site + Jd + I(Jd2)+Site*Jd)	9	644.62	1.92	0.18	0.83
$\lambda(.)\gamma(.)\omega(.)$[Ricker]$p$(Site + Jd + I(Jd2)+Site*Jd)	9	644.64	1.93	0.17	1

Table 3
Model averaged parameter estimates for black rhino: detection probability (p) recruitment rate, (γ) growth rate, and (ω) carrying capacity in Madikwe and Pilanesberg (B), South Africa (1999-2015). (*) Growth rate and carrying capacity are estimated using the Ricker models.

	Estimates	SE
Detection		
Intercept p (.)	0.10	0.21
p (SiteB)	1.16	0.23
p (Julian date)	0.14	0.07
p (Julian date2)	−0.10	0.04
p (Julian date*SiteB)	−0.43	0.15
Growth Rate:		
Intercept γ (.)	−0.96	0.56
γ (Rain)	0.67	0.63
γ (Temp)	−0.06	0.19
Carrying Capacity:		
Intercept ω (.)	4.29	0.08

3.2. Detection, population size and trend

The relation between Julian date and detection probability shows that detection declines in September and October, during early green-up of woody vegetation. Detectability was close to one in Pilanesberg for the earliest dates, while it was approximately 0.8 in Madikwe at the same time and diminished thereafter. There was a difference in detectability between both reserves: at the end of September, detectability decreased in both areas, although more markedly in Pilanesberg (Fig. 3 and Table 3).

There is some support for effects of precipitation and temperature on growth rate, although it is weak (Table 3). Population size in Madikwe and Pilanesberg showed similar dynamics (Fig. 4), with a density range of 0.078–0.098 and 0.139–0.142 individuals/km^2, respectively. Carrying capacity based on the Ricker model in unmarked (Fig. 4 and Table 3) was estimated as 73.07 (60.99–85.14) individuals, or a density of ca. 0.122 (0.102–0.142) individuals/100 km^2. The population size estimates using the model DDSR in a Bayesian approach (Bellier et al., 2016) are somewhat similar to those obtained using the unmarked model (Results in Appendix C vs Abundance in Appendix A). The average difference in estimates between Bayesian vs unmarked approaches was 2.2 (1.57–6.84) individuals (positive) for Madikwe, and 1.80 (4.45–0.07) individuals for Pilanesberg (negative).

3.3. Goodness of fit

The bootstrap *p*-values for the best-fit model based on the SSE, Freeman-Tukey, and Chi-square statistics were 0.66, 0.69 and 0.67, respectively, suggesting that our model provided an adequate fit to the data (Figure A2 in Appendix 2). The value of $\hat{c}$ (ratio of observed/expected) was 0.73, indicating a slight under-dispersion.

3.4. Simulations

Using a simulated time span of 20 years (Table 4 and Appendix D), the estimate of initial abundance (λ) using N-mixture models had root-mean-square error (RSME) values substantially lower than using maximum yearly counts. For density-

Fig. 2. Black rhino group sighted in the bushveld during the aerial counts in Madikwe Game Reserve (Source: NWPTB, 2015).

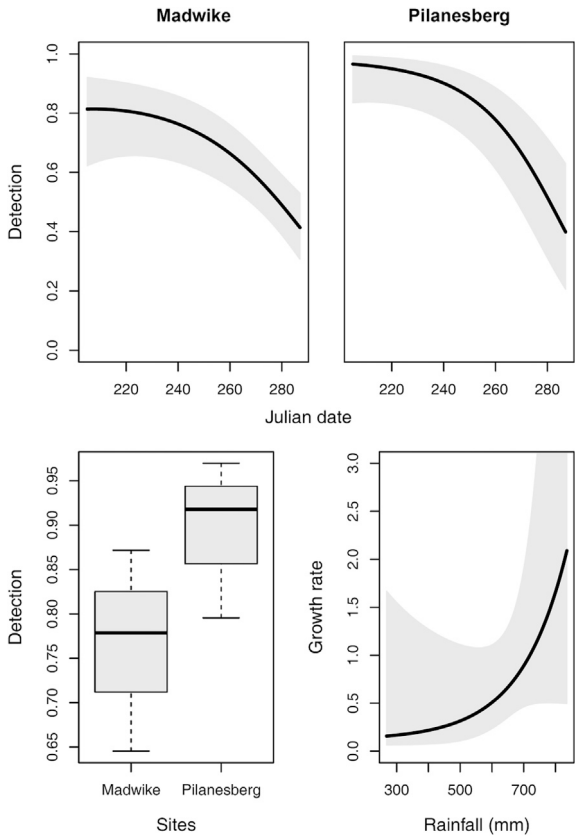

Fig. 3. Predictions using model averaging from the best-fit models (ΔAICc<2). Top: probability of detecting black rhino in Madikwe and Pilanesberg depending on Julian date. Bottom left: detection probability by Site. Bottom right: growth rate vs. rainfall ( ). Mean estimates are in black and their 95% confidence intervals are in grey.

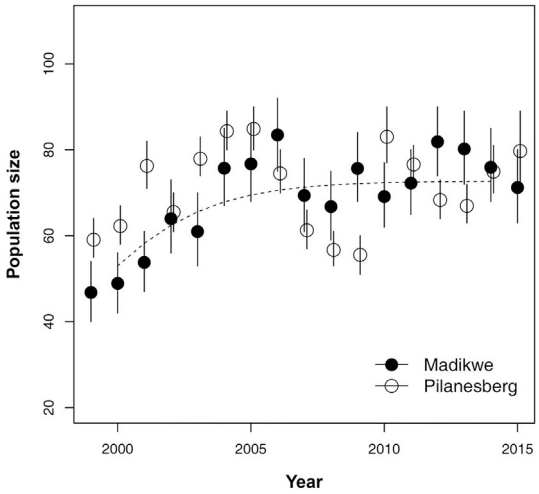

Fig. 4. Average estimated abundance of Black Rhinoceros *Diceros bicornis* in Madikwe and Pilanesberg in 1999–2015 and Ricker model fit (dashed). Bars represent 95% confidence intervals on abundance estimates.

Table 4
Root-mean-square error (RMSE) from the population parameter estimates through simulations. Simulations are based on our parameters estimates from the null models for Ricker and constant dynamics, for $M \in \{2, 5, 10\}$ spatial replicates (sites). We also compare the RMSE from estimates and from raw count data (using the maximum from three yearly replicates). One hundred simulations of each case were conducted. Parameters: lambda: initial abundance; gamma: recruitment rate (constant) or growth rate (Ricker); omega: apparent survival probability (constant) or equilibrium abundance (Ricker) and p: detection probability.

M	Parameter	RICKER			CONSTANT		
		Simulated	RMSE		Simulated	RMSE	
			Estimates	Counts		Estimates	Counts
2	*lambda* (λ)	62.00	6.75	22.36	58.00	7.38	23.19
	gamma (γ)	0.20	0.15		21.00	8.93	
	omega (ω)	88.00	10.23		0.73	0.12	
	p	0.60	0.05		0.60	0.09	
5	*lambda* (λ)	62.00	5.12	20.74	58.00	6.16	17.10
	gamma (γ)	0.20	0.08		21.00	5.11	
	omega (ω)	88.00	6.71		0.73	0.06	
	p	0.60	0.04		0.60	0.04	
10	*lambda* (λ)	62.00	4.00	21.93	58.00	3.58	21.00
	gamma (γ)	0.20	0.05		21.00	3.07	
	omega (ω)	88.00	5.44		0.73	0.04	
	p	0.60	0.03		0.60	0.03	

dependent and constant dynamics, the RMSE was reduced by half if we used ten spatial replicates instead of two. The accuracy of the detection probability estimate was high in both the constant and the Ricker models; however, in the simulation with density dependence, the accuracy of growth rate was lower than for the constant model.

3.5. Comparison of RMG ID and N-mixture estimates

The range in RMG ID estimates for Madikwe was 27–82 with an average (1999-2015) of 56.5. For the N-mixture estimates, the minimum was 46.8 (40-54), the maximum was 83.5 (75-92), and the average (1999-2015) was 69.0 (53-85). The N-mixture average estimate was 22.2% higher. The RMG estimates for Pilanesberg ranged from 48 to 66 with an average of 56.0. The N-mixture estimates had a minimum of 55.6 (51-60), a maximum of 84.9 (80-90), and an average (1999-2015) of 71.09 (61-81). N-mixture average estimate was 26.7% higher than of RMG.

4. Discussion

The density estimates we obtained from this study were between 0.078 and 0.154 rhinos/km^2 which were similar to the density estimates reported in Pilanesberg (0.076 individuals/km^2) by Adcock et al. (1998), who also pointed out that this population was then still below its ecological carrying capacity. Model selection for the N-mixture model also allowed us to

confirm that density-dependent processes were evident for these populations of black rhino. AIC supported density-dependent models, with three of the four best models including Ricker distributions (Table 3). This selected distribution described a rapidly growing population with a horizontal asymptote of 0.122 (0.102–0.142) individuals/km^2. (Fig. 4). The estimates of population size and support for density dependence that we obtained using the DDSR model were similar (see Fig. 4 and Fig. C1 from Appendix C) to those based on model selection in unmarked.

While the growth rate estimates from our model require cautious interpretation (Bellier et al., 2016), we found evidence that rainfall has had a positive effect on the growth rate (Fig. 3, Table 3). Therefore, it is expected that rainfall positively influences black rhino populations. For instance, Berkeley and Linklater (2010) indicated that rainfall and, therefore, range conditions around conception influence seasonal conception rates and seasonal and annual progeny sex ratios.

In general, estimates from N-mixture models could be improved by using more spatial replicates (Knape and Korner-Nievergelt, 2015), although short time series from many sites can yield estimates of similar accuracy as long series from few sites (Bellier et al., 2016), as in our study. This is consistent with the results of our simulations (Table 4 and Appendix D). Furthermore, the use of more covariates would give further insights on the population responses to different observational and environmental conditions.

The use of N-mixture models with aerial count data may provide an instrumental framework for species management, which would allow managers to obtain better population estimates. Even in complex situations like those involving density-dependence and environmental stochasticity, abundance and detection probability can be more accurately estimated, as demonstrated by our simulation. To improve the accuracy of vital rates estimates we could use a Bayesian N-mixture approach, select the appropriate type of density-dependence (DDR, DDS or DDSR) (Bellier et al., 2016) and also use informative priors. Vital rate estimates could be also addressed using identification-based models or even integrated population models (e.g. combining spatial capture-recapture and count models) that have important advantages compared to conventional analyses (Schaub et al., 2007) to obtain unbiased estimates.

About the differences of detection probability between reserves, SDAC RMG using ID monitoring (personal communication, April 4, 2019) found that a greater proportion of the population is counted in Pilanesberg than Madikwe, as we found using N-mixture model (Fig. 3). In contrast, the differences in abundance between RMG ID and N-mixture estimates were unexpected. If we assume RMG ID are unbiased, the differences could lie in the execution of the aerial surveys. Accidental double-counts can lead to overestimation because a substantial bias arises with only a slight violation of model assumptions (Link et al., 2018). Another cause of bias could be an unmodeled source of variation in detection (e.g. observer experience). In the future, such biases could be minimized through proper planning, training and execution. Furthermore, integrated population models (IPM) or N-mixture models that incorporate false positives and false-negatives could reduce the effect of double-counting (Chambert et al., 2016). The use of those models is an attractive and simple approach to estimate densities of large mammals besides black rhino in the region, and they facilitate working at scales that are relevant for conservation and management. Aerial counts of large mammals, and the application of N-mixture models, would improve population size estimates, and provide more accurate knowledge of population trends and uncertainty of estimates. It should be noted that according our simulations (Table 4) even with high detection probability, the use of raw counts could mask substantial fluctuations in population sizes. In our simulations, using a detection probability of 0.6 and three replicates, maximum counts are biased at a 30%. Furthermore, an additional advantage of using dynamic N-mixture models is the possibility to include covariates as potential predictors of recruitment, survival and species abundance. Evaluating the relationship between potential covariates and demographic vital rates could provide more comprehensive information, which could aid in identifying threats to a species and could be targeted by the policy-making authorities.

Acknowledgements

We thank Mpho Ellen Sekgarametso of North West Parks and Tourism Board, and NASA Prediction of Worldwide Energy Resources for aiding with access to data, and to Edwige Bellier and Marc Kéry for providing us their complete Bayesian codes in JAGS.

Jose Jimenez is funded by Plan TIFIES (*Spanish Action Plan against illegal trafficking and international poaching of wild species*). Ministerio para la Transición Ecológica. Government of Spain.

Appendix A. Supplementary data

Supplementary data to this article can be found online at https://doi.org/10.1016/j.gecco.2019.e00687.

References

Acocks, J.P.H., 1975. Veld Types of South Africa. Memoirs of the Botanical Survey of South Africa, No. 40. Botanical Research Institute, Department of Agricultural Technical Services, Pretoria, Republic of South Africa.

Adcock, K., 1994. The relevance of "territorial" behaviour in black rhino to their population management. In: Proc. A Symp. Rhinos as Game Ranch Anim. Onderstepoort, Repub. South Africa.

Adcock, K., Hansen, H.B., Lindemann, H., 1998. Lessons from the introduced black rhino population in Pilanesberg National Park. PACHYDERM 40–51.

Akaike, H., 1974. A new look at statistical model identification. IEEE Trans. Autom. Control 19, 716–723.

Amin, R., Thomas, K., Emslie, R.H., Foose, T.J., Van Strien, N.V., 2006. An overview of the conservation status of and threats to rhinoceros species in the wild. Int. Zoo Yearb. 40, 96–117. https://doi.org/10.1111/j.1748-1090.2006.00096.x.
Bellier, E., Kéry, M., Schaub, M., 2016. Simulation-based assessment of dynamic N-mixture models in the presence of density dependence and environmental stochasticity. Methods Ecol. Evol. 7, 1029–1040. https://doi.org/10.1111/2041-210X.12572.
Berger, J., 1994. Conservation, and black rhinos. J. Mammal. 75, 298–308. https://doi.org/10.1644/826.1.Key.
Berkeley, E.V., Linklater, W.L., 2010. Annual and seasonal rainfall may influence progeny sex ratio in the black rhinoceros. S. Afr. J. Wildl. Res. 40, 53–57. https://doi.org/10.3957/056.040.0102.
Brockett, B.H., 2002. Accuracy, bias and precision of helicopter-based counts of black rhinoceros in Pilanesberg National Park, South Africa. S. Afr. J. Wildl. Res. 32, 121–136.
Brooks, M., Emslie, R., 1999. African Rhino. Status Survey and Conservation Action Plan. Gland, Switzerland and Cambridge, UK.
Burnham, K.P., Anderson, D.R., 2002. Model Selection and Multimodel Inference: A Practical Information-Theoretic Approach, second ed. Springer Verlag, New York https://doi.org/10.1007/b97636.
Carruthers, J., 2011. Pilanesberg national park, North West Province, South Africa: uniting economic development with ecological design – a history, 1960s to 1984. Koedoe 53, 1–10. https://doi.org/10.4102/koedoe.v53i1.1028.
Caughley, G., 1977. Sampling in aerial survey. J. Wildl. Manag. 41, 605–615. https://www.jstor.org/stable/3799980.
Chambert, T., Hossack, B.R., Fishback, L.A., Davenport, J.M., 2016. Estimating abundance in the presence of species uncertainty. Methods Ecol. Evol. 7, 1041–1049. https://doi.org/10.1111/2041-210X.12570.
Chandler, R.B., King, D.I., 2011. Habitat quality and habitat selection of golden-winged warblers in Costa Rica: an application of hierarchical models for open populations. J. Appl. Ecol. 48, 1038–1047. https://doi.org/10.1111/j.1365-2664.2011.02001.x.
Chandler, R.B., 2018. Unmarked. GitHub Repos. WWW Document] URL: https://github.com/rbchan/unmarked/blob/master/inst/unitTests/sim.pcountOpen.r#L742. (Accessed 20 December 2018). accessed.
Cromsigt, J.P.G.M., Hearne, J., Heitkönig, I.M.A., Prins, H.H.T., 2002. Using models in the management of Black rhino populations. Ecol. Model. 149, 203–211. https://doi.org/10.1016/S0304-3800(01)00524-5.
Dail, D., Madsen, L., 2011. Models for estimating abundance from repeated counts of an open metapopulation. Biometrics 67, 577–587. https://doi.org/10.1111/j.1541-0420.2010.01465.x.
De Valpine, P., Turek, D., Paciorek, C.J., Anderson-Bergman, C., Lang, D.T., Bodik, R., 2017. Programming with models: writing statistical algorithms for general model structures with NIMBLE. J. Comput. Graph. Stat. 26, 403–413. https://doi.org/10.1080/10618600.2016.1172487.
Emslie, R., Adcock, K., 2016. A Conservation Assessment of Diceros bicornis. Red List Mamm. South Africa, Swazil. Lesotho, p. 32.
Emslie, R.H., 2012. Diceros bicornis Ssp. Minor. WWW Document]. IUCN Red List Threat. Species. https://doi.org/10.2305/IUCN.UK.2012.RLTS.T39321A16981557.en. (Accessed 1 December 2018). accessed.
Farrell, Van Riet, Tinley, K.L., 1978. Pilanesberg National Park, Bophuthatswana: Planning and Management Proposals for Department of Agriculture, Republic of Bophuthatswana, August 1978 (unpublished report).
Ferreira, S.M., Bisset, C., Cowell, C., Gaylard, A., Greaver, C., Hayes, J., van der Vyver, L., Zimmerman, D., 2017. The status of rhinoceroses in South African National Parks. Koedoe 1–11. https://doi.org/10.4102/koedoe.v59i1.1392.
Ferreira, S.M., Greaver, C.C., Knight, M.H., 2011. Assessing the population performance of the black rhinoceros in Kruger national park. S. Afr. J. Wildl. Res. 41, 192–204. https://doi.org/10.3957/056.041.0206.
Fiske, I.J., Chandler, R.B., 2011. unmarked: an R package for fitting hierarchical models of wildlife occurrence and abundance. J. Stat. Softw. 43, 1–23. https://doi.org/10.1002/wics.10.
Foose, T.J., Lacy, R.C., Brett, R., Seal, U.S., 1993. Kenya Black Rhino Metapopulation Workshop Part 2. IUCN/SSC Captive Breeding Specialist Group (CBSG), Apple Valley.
Freeman, E.W., Meyer, J.M., Bird, J., Adendorff, J., Schulte, B.A., Santymire, R.M., 2014. Impacts of environmental pressures on the reproductive physiology of subpopulations of black rhinoceros (Diceros bicornis bicornis) in Addo Elephant National Park, South Africa. Conserv. Physiol. 2, 1–13. https://doi.org/10.1093/conphys/cot034.
Gakahu, C.G., 1993. African rhinos: current numbers and distribution. In: Proceedings of an International Conference. Zoological Society, San Diego, U.S.A., pp. 161–165
Gimenez, O., Viallefont, A., Charmantier, A., Pradel, R., Cam, E., Brown, C.R., Anderson, M.D., Brown, M.B., Covas, R., Gaillard, J., 2008. The risk of flawed inference in evolutionary studies when detectability is less than one. Am. Nat. 172, 441–448. https://doi.org/10.1086/589520.
Hanski, I., 2006. Density dependence, regulation and variability in animal populations. Philos. Trans. R. Soc. London. Biol. Sci. 330, 141–150. https://doi.org/10.1098/rstb.1990.0188.
Hone, J., 2008. On bias, precision and accuracy in wildlife aerial surveys. Wildl. Res. 35, 253–257. https://doi.org/10.1071/WR07144.
Hostetler, J.A., Chandler, R.B., 2015. Improved state-space models for inference about spatial and temporal variation in abundance from count data. Ecology 96, 1713–1723. https://doi.org/10.1890/14-1487.1.
Hrabar, H., du Toit, J.T., 2005. Dynamics of a protected black rhino (Diceros bicornis) population: Pilanesberg National Park, South Africa. Anim. Conserv. 8, 259–267. https://doi.org/10.1017/S1367943005002234.
Jachmann, H., 2002. Comparison of aerial counts with ground counts for large African herbivores. J. Appl. Ecol. 39, 841–852. https://doi.org/10.1046/j.1365-2664.2002.00752.x.
Kéry, M., Dorazio, R.M., Soldaat, L., van Strien, A., Zuiderwijk, A., Royle, J.A., 2009. Trend estimation in populations with imperfect detection. J. Appl. Ecol. 46, 1163–1172. https://doi.org/10.1111/j.1365-2664.2009.01724.x.
Kéry, M., Schaub, M., 2012. Bayesian Population Analysis Using WinBUGS. A Hierarchical Perspective. Academic Press/Elsevier. https://doi.org/10.1016/B978-0-12-387020-9.00014-6.
King, J.M., Sayers, A.R., Chara, P., de Leeuw, P.N., Peacock, C.P., 1985. Improving aerial counts of Maasai livestock. Agric. Syst. 16, 231–256. https://doi.org/10.1016/0308-521X(85)90062-9.
Knape, J., Korner-Nievergelt, F., 2015. Estimates from non-replicated population surveys rely on critical assumptions. Methods Ecol. Evol. 6, 298–306. https://doi.org/10.1111/2041-210X.12329.
Link, W.A., Schofield, M.R., Barker, R.J., Sauer, J.R., 2018. On the robustness of N-mixture models. Ecology 99, 1547–1551. https://doi.org/10.1002/ecy.2362.
Lundberg, P., Ranta, E., Ripa, J., Kaitala, V., 2000. Population variability in space and time. Trends Ecol. Evol. 15, 460–464. https://doi.org/10.1016/S0169-5347(00)01981-9.
Lyet, A., Slabbert, R., Versfeld, W.F., Leslie, A.J., Beytell, P.C., Preez, P. Du, 2016. Using a binomial mixture model and aerial counts for an accurate estimate of nile crocodile abundance and population size in the Kunene river, Namibia. African J. Wildl. Res. 46, 71–86. https://doi.org/10.3957/056.046.0071.
MacKenzie, D.I., Nichols, J.D., Royle, J.A., Pollock, K.H., Bailey, L.L., Hines, J.E., 2006. Occupancy Estimation and Modeling. Inferring Patterns and Dynamics of Species Occurrence, Statewide Agricultural Land Use Baseline 2015. Elsevier Inc. https://doi.org/10.1017/CBO9781107415324.004.
Mackie, C.S., Dunham, K.M., Ghiurghi, A., 2013. Current status and distribution of the Vulnerable common hippopotamus Hippopotamus amphibius in Mozambique. Oryx 47, 70–76. https://doi.org/10.1017/S0030605311001554.
Martin, E.B., 1991. The present-day trade routes and markets for rhinoceros products. In: Proc. Int. Conf. Rhinoceros Biol. Conserv. San Diego, pp. 1–10.
Martin, J., Royle, J.A., Mackenzie, D.I., Edwards, H.H., Kéry, M., Gardner, B., 2011. Accounting for non-independent detection when estimating abundance of organisms with a Bayesian approach. Methods Ecol. Evol. 2, 595–601. https://doi.org/10.1111/j.2041-210X.2011.00113.x.
Martin, T.E., Clobert, J., Anderson, D.R., 1995. Return rates in studies of life history evolution: are biases large? J. Appl. Stat. 22, 863–876. https://doi.org/10.1080/02664769524676.

McCarthy, M.A., Possingham, H.P., 2007. Active adaptive management for conservation. Conserv. Biol. 21, 956–963. https://doi.org/10.1111/j.1523-1739.2007.00677.x.
McCarthy, T., Rubidge, B., 2006. The Story of Earth & Life. Struik Publishers (Pty) Ltd, Cape Town, South Africa.
Mduma, S.A.R., Sinclair, A.R.E., Hilborn, R., 1999. Food regulates the Serengeti wildebeest: a 40-year record. J. Anim. Ecol. 68, 1101–1122. https://doi.org/10.1046/j.1365-2656.1999.00352.x.
Moilanen, A., 2002. Implications of empirical data quality to metapopulation model parameter estimation and application. Oikos 96, 516–530. https://doi.org/10.1034/j.1600-0706.2002.960313.x.
Moodley, Y., Russo, I.R.M., Dalton, D.L., Kotzé, A., Muya, S., Haubensak, P., Bálint, B., Munimanda, G.K., Deimel, C., Setzer, A., Dicks, K., Herzig-Straschil, B., Kalthoff, D.C., Siegismund, H.R., Robovský, J., O'Donoghue, P., Bruford, M.W., 2017. Extinctions, genetic erosion and conservation options for the black rhinoceros (Diceros bicornis). Sci. Rep. 7, 1–16. https://doi.org/10.1038/srep41417.
Mucina, L., Rutherford, M.C., 2006. The Vegetation of South Africa, Lesotho and Swaziland, vol. 19. Strelitzia, Strelitzia.
NASA, 2018. Prediction of Worldwide Energy Resources [WWW Document] URL. https://power.larc.nasa.gov/. (Accessed 22 October 2018). accessed.
Nel, H.P., 2015. Population Estimates for Large Herbivores and Predators in Protected Areas in the North West Parks Board.
Nichols, J.D., Boulinier, T., Hines, J.E., Pollock, K.H., Sauer, J.R., 1998. Inference methods for spatial variation in species richness and community composition when not all species are detected. Conserv. Biol. 12, 1290–1298. https://doi.org/10.1016/S0140-6736(00)79589-4.
Nichols, J.D., Williams, B.K., 2006. Monitoring for conservation. Trends Ecol. Evol. 21, 668–673. https://doi.org/10.1016/j.tree.2006.08.007.
NIMBLE Development Team, 2018. NIMBLE User Manual [WWW Document]. URL. https://r-nimble.org/html_manual/. (Accessed 10 November 2018). accessed.
NWPTB, 2015. Pilanesberg National Park Management Plan. Draft for Discussion.
NWPTB, 2018. North West Parks Board Official Website. WWW Document]. URL https://www.northwestparks.org.za. (Accessed 22 September 2018). accessed.
Ottichilo, W.K., 1999. Comparison of sample and total counts of elephant and buffalo in Masai Mara, Kenya. Afr. J. Ecol. 37, 435–438. https://doi.org/10.1046/j.1365-2028.1999.00199.x.
Owen-Smith, N., 1990. Demography of a large herbivore, the Greater Kudu Tragelaphus strepsiceros, in relation to rainfall. J. Anim. Ecol. 59, 893–913. https://doi.org/10.2307/5021.
Parker, G., Sundaresan, S., Chege, G., O'Brien, T., 2011. Using sample aerial surveys to estimate the abundance of the endangered Grevy's zebra in northern Kenya. Afr. J. Ecol. 49, 56–61. https://doi.org/10.1111/j.1365-2028.2010.01232.x.
R Core Team, 2018. R: A Language and Environment for Statistical Computing. R Foundation for Statistical Computing.
Ricker, W.E., 1958. A handbook of computations for biological statistics of fish populations. Fish. Res. Board Can. Bull. 1, 119.
Ricker, W.E., 1954. Stock and recruitment. J. Fish. Res. Board Can. 11, 559–623.
Royle, J.A., 2004. N-mixture models for estimating population size from spatially replicated counts. Biometrics 60, 108–115. https://doi.org/10.1111/j.0006-341X.2004.00142.x.
Sæther, B.E., 1997. Environmental stochasticity and population dynamics of large herbivores: a search for mechanisms. Trends Ecol. Evol. 12, 143–147. https://doi.org/10.1016/S0169-5347(96)10068-9.
Schaub, M., Gimenez, O., Sierro, A., Arlettaz, R., 2007. Use of integrated modeling to enhance estimates of population dynamics obtained from limited data. Conserv. Biol. 21, 945–955. https://doi.org/10.1111/j.1523-1739.2007.00743.x.
Schmidt, B.R., 2005. Monitoring the distribution of pond-breeding amphibians when species are detected imperfectly. Aquat. Conserv. Mar. Freshw. Ecosyst. 15, 681–692. https://doi.org/10.1002/aqc.740.
Sinclair, a R.E., Dublin, H., Borner, M., 1985. Population regulation of serengeti wildebeest: a rest of the food hypothesis. Oecologia 65, 266–268. https://doi.org/10.1007/BF00379227.
Skalski, J.R., 1994. Estimating wildlife populations based on incomplete area surveys. Wildl. Soc. Bull. 22, 192–203. http://www.jstor.org/stable/3783246.
Steinhorst, R.K., Samuel, M.D., 1989. Sightability adjustment methods for aerial surveys of wildlife populations. Int. Biometric Soc. 45, 415–425. https://www.jstor.org/stable/2531486.
Tyre, A.J., Tenhumberg, B., Field, S.A., Niejalke, D., Possingham, H.P., 2003. Improving precision and reducing bias in biological surveys: estimating false-negative error rates. Ecol. Appl. 13, 1790–1801. https://doi.org/10.1890/02-5078.
Walpole, M.J., Morgan-Davies, M., Milledge, S., Bett, P., Leader-Williams, N., 2001. Population dynamics and future conservation of a free-ranging black rhinoceros population in Kenya. Biol. Conserv. 99, 143–237. https://doi.org/10.1016/S0006-3207(00)00219-6.
Wiest, W.A., Correll, M.D., Marcot, B.G., Olsen, B.J., Elphick, C.S., Hodgman, T.P., Guntenspergen, G.R., Shriver, W.G., 2018. Estimates of tidal-marsh bird densities using Bayesian networks. J. Wildl. Manag. 1–12. https://doi.org/10.1002/jwmg.21567.
Williams, P.J., Hooten, M.B., Womble, J.N., Bower, M.R., 2017. Estimating occupancy and abundance using aerial images with imperfect detection. Methods Ecol. Evol. 8, 1679–1689. https://doi.org/10.1111/2041-210X.12815.